EFFECT OF DAMAGE ON THE CRACK-TIP FIELD IN POWER-LAW MATERIALS

D. GROSS and Ch. ZHANG
Institute of Mechanics, TH Darmstadt
W-6100 Darmstadt, Germany

ABSTRACT

Asymptotic crack-tip field is analyzed for a Mode III crack in a power-law material containing a distribution of micro-cracks (damage). Constitutive equations for the overall macroscopic strains and stresses are derived via a homogenization-technique. Asymptotic analysis is performed for the crack-tip field by solving a nonlinear eigenvalue problem. Numerical results are presented to explore the effect of damage on the crack-tip field.

KEYWORDS

Crack-tip field, damage, micro-mechanics.

INTRODUCTION

The stress and strain distributions near a pre-existing macro-crack tip may be considerably altered by the presence of micro-cracks or micro-voids (damage) in the immediate neighbourhood of the macro-crack tip. For assesing the initiation and growth of a macro-crack, a realistic model should take the influence of this kind of damage into account. In this paper, a stationary and semi-infinite Mode III macro-crack in a power-law solid containing distributed micro-cracks, here regarded as microstructural damage, is investigated. The micro-cracks are assumed to be randomly located but non-randomly oriented. Thus, the damage considered in this analysis has an anisotropic nature, and the associated overall macroscopic behavior of the damaged solid is also anisotropic. Constitutive equations for the macroscopic strains and stresses are obtained by a homogenization-technique, under the assumption of geometrically identical micro-cracks with a dilute concentration. An asymptotic analysis is performed for the near-tip field of a macro-crack by solving the corresponding nonlinear eigenvalue problem. It is shown that the crack-tip field of the damaged solid has the same structure as the Mode III HRR-field (Hutchinson, 1968; Rice and Rosengren, 1968) of the undamaged solid, under the assumptions made in this analysis. Numerical results are presented to reveal the effect of microstructural damage on the angular functions, the contours of constant effective shear stress, the normalization constant appearing in the crack-tip field, and the crack opening displacement.

CONSTITUTIVE EQUATIONS

Let us consider a homogeneous, isotropic, and power-law solid containing a random distribution of micro-cracks. The solid is assumed to be in a state of anti-plane strain. Hence, the only non-zero displacement component w is in the x_3-direction, and the non-vanishing strain and stress components are γ_α and τ_α, where α =1 and 2. The undamaged (unmicro-cracked) solid is characterized by the following complementary potential function

$$\Psi_0 = \alpha\gamma_0\tau_0(\frac{\tau_e}{\tau_0})^{n+1}\frac{1}{n+1}, \tag{1}$$

where τ_0 is a reference shear stress and γ_0 is a reference shear strain, α is a dimensionless material constant, n is the material hardening exponent varying from unity for linear-elastic solid to infinity for rigid ideal-plastic solid, and τ_e is the effective shear stress defined by

$$\tau_e = (\tau_\alpha\tau_\alpha)^{1/2}. \tag{2}$$

The presence of distributed micro-cracks gives rise to a change in the complementary potential function Ψ for the overall macroscopic strains and stresses. It is assumed in this analysis that the spacing of micro-cracks is sufficiently large so that interaction effects among them can be neglected. It is further assumed that all the micro-cracks have the same length $2a$ and they are oriented parallel to each other. Under these assumptions and by using the commonly applied homogenization technique, the total change of the complementary potential function can be approximated by

$$\Psi_c = 2\rho\int_0^a J(a)da, \tag{3}$$

where ρ denotes the number density of the micro-cracks (number of micro-cracks per unit area) and $J(a)$ is the J-integral (Rice, 1968) of an isolated anti-plane micro-crack in an infinite power-law solid. Although analytical result for $J(a)$ is available (Amazigo, 1974), it is difficult to implement this result into the present formulation, since the analytical expression for $J(a)$ is extremly complicated. For simplicity, an approximate formula for $J(a)$ is used here, which can be obtained by using a perturbation method (Abeyaratne, 1983; He, 1987; Zhang and Gross, 1991). The result is

$$J(a) \simeq \frac{\sqrt{n}}{2}\pi a\alpha\gamma_0\tau_0(\frac{\tau_e}{\tau_0})^{n+1}(\frac{\tau_2\cos\phi - \tau_1\sin\phi}{\tau_e})^2, \tag{4}$$

where ϕ is the orientation angle of the micro-crack with respect to the global coordinate system. Note here that Eq. (4) is exact for n=1, i.e., linearly elastic solid. Substitution of Eq. (4) into Eq. (3) yields

$$\Psi_c = \frac{\sqrt{n}}{2}\rho\pi a^2\alpha\gamma_0\tau_0(\frac{\tau_e}{\tau_0})^{n+1}(\frac{\tau_2\cos\phi - \tau_1\sin\phi}{\tau_e})^2. \tag{5}$$

The total complementary potential function of the damaged solid can be written as

$$\Psi = \Psi_0 + \Psi_c = \alpha\gamma_0\tau_0(\frac{\tau_e}{\tau_0})^{n+1}\frac{1}{n+1}[1 + \omega\pi(n+1)\frac{\sqrt{n}}{2\tau_e^2}(\tau_2\cos\phi - \tau_1\sin\phi)^2], \tag{6}$$

where $\omega = \rho a^2$ is the crack density parameter which is regarded as a damage parameter in the present analysis. By using Eq. (6) the constitutive equations for the damaged solid can be immediately obtained as

$$\gamma_\alpha = \frac{\partial\Psi}{\partial\tau_\alpha} = \alpha\gamma_0(\frac{\tau_e}{\tau_0})^{n-1}\frac{\tau_1}{\tau_0}[1 + f_\alpha], \tag{7}$$

in which

$$f_1 = \omega\pi\frac{\sqrt{n}}{2\tau_e^2}\{(n+1)(\tau_2\cos\phi - \tau_1\sin\phi)^2 - \frac{\tau_2}{\tau_1}[(\tau_2^2 - \tau_1^2)\sin 2\phi + 2\tau_1\tau_2\cos 2\phi]\}, \tag{8}$$

$$f_2 = \omega\pi\frac{\sqrt{n}}{2\tau_e^2}\{(n+1)(\tau_2\cos\phi - \tau_1\sin\phi)^2 + \frac{\tau_1}{\tau_2}[(\tau_2^2 - \tau_1^2)\sin 2\phi + 2\tau_1\tau_2\cos 2\phi]\}. \tag{9}$$

It should be noted here that the damage state is characterized by both the damage density parameter ω and the damage orientation parameter ϕ. Hence, the damage considered here has an anisotropic character. Consequently, the overall macroscopic property of the damaged solid is also anisotropic, as can be directly recognized on Eq. (7).

CRACK-TIP FIELD

Consider now a stationary and semi-infinite Mode III macro-crack in a power-law solid containing a distribution of micro-cracks. In general, the damage or the micro-crack density parameter ω should decay with increasing distance from the macro-crack tip. In this analysis, however, it is assumed that the distribution of micro-cracks is approximately uniform near the macro-crack tip so that the damage parameter ω can be regarded as constant. Small strain theory is used here, and the damaged solid is characterized by the constitutive equations (7).

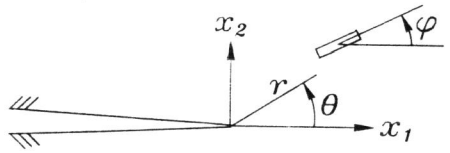

Figure 1: Polar coordinate system

For convenience, a polar coordinate system (r,θ) with origin at the macro-crack tip is introduced, as shown in Fig. 1. In the polar coordinate system, the equilibrium equation can be written as

$$\frac{\partial(r\tau_r)}{\partial r} + \frac{\partial\tau_\theta}{\partial\theta} = 0, \tag{10}$$

while the compatibility equation may be stated as

$$\frac{\partial(r\gamma_\theta)}{\partial r} - \frac{\partial\gamma_r}{\partial\theta} = 0. \tag{11}$$

To perform an asymptotic stress analysis at the macro-crack tip, a stress function F is introduced, which is related to the stress components by

$$\tau_r = -\frac{1}{r}\frac{\partial F}{\partial \theta}, \qquad \tau_\theta = \frac{\partial F}{\partial r}. \tag{12}$$

With Eq. (12), the equilibrium equation is identically satisfied. It is assumed that near the macro-crack tip, i.e., for $r \to 0$, the stress function can be expressed in a separated form as

$$F = -A\tau_0 r^s \bar{F}(\theta), \tag{13}$$

where A is an amplitude factor, and s is an exponent to be determined. Equation (22) with Eq. (13) together results in

$$\tau_r = -A\tau_0 r^{s-1}\bar{F}'(\theta), \qquad \tau_\theta = A\tau_0 s r^{s-1}\bar{F}(\theta), \tag{14}$$

$$\tau_e = A\tau_0 r^{s-1}\bar{\tau}_e(\theta), \qquad \bar{\tau}_e(\theta) = (\bar{F}'^2 + s^2\bar{F}^2)^{1/2}, \tag{15}$$

in which $(\cdot)' = \partial(\cdot)/\partial\theta$. Substitution of Eqs. (14) and (15) into the constitutive equations (7) and subsequently into the compatibility equation (11) yields the following nonlinear ordinary differential equation

$$\begin{aligned}
&\{(n-1)\bar{F}'(\bar{F}'+p) + \bar{\tau}_e^2 - 2\bar{F}'p + \omega\pi\frac{\sqrt{n}}{2}[(n+1)M^2 + 2(n+1)\bar{F}'M\sin(\theta-\phi) + \\
&2s\bar{F}(\bar{F}'\sin(2\theta-2\phi) - s\bar{F}\cos(2\theta-2\phi))]\}\bar{F}'' + s^2(n-1)\bar{F}\bar{F}'(\bar{F}'+p) + \\
&[(s-1)n+1]\bar{\tau}_e^2(s\bar{F}+q) - 2s^2\bar{F}\bar{F}'p + \omega\pi\frac{\sqrt{n}}{2}\{2(n+1)\bar{F}'M[(1-s)\times \\
&\bar{F}'\cos(\theta-\phi) + s\bar{F}\sin(\theta-\phi)] + s\bar{F}'N + 2s\bar{F}[(1-s)\bar{F}'^2 - s^2\bar{F}^2]\times \\
&\cos(2\theta-2\phi) + 2s^2(2-s)\bar{F}^2\bar{F}'\sin(2\theta-2\phi)\} = 0,
\end{aligned} \tag{16}$$

where

$$M(\theta) = \bar{F}'\sin(\theta-\phi) - s\bar{F}\cos(\theta-\phi), \tag{17}$$

$$N(\theta) = (\bar{F}'^2 - s^2\bar{F}^2)\sin(2\theta-2\phi) - 2s\bar{F}\bar{F}'\cos(2\theta-2\phi), \tag{18}$$

$$p(\theta) = \omega\pi\frac{\sqrt{n}}{2\bar{\tau}_e^2}[(n+1)\bar{F}'M^2(\theta) + s\bar{F}N(\theta)], \tag{19}$$

$$q(\theta) = \omega\pi\frac{\sqrt{n}}{2\bar{\tau}_e^2}[(n+1)s\bar{F}M^2(\theta) - \bar{F}'N(\theta)]. \tag{20}$$

The nonlinear differential equation (16) in conjunction with the boundary conditions

$$\bar{F}(\pi) = 0, \quad \bar{F}(-\pi) = 0, \quad \bar{F}'(-\pi) = 1, \tag{21}$$

forms a nonlinear eigenvalue problem for determining the eigenvalue s and the eigenfunction $\bar{F}(\theta)$. The first two boundary conditions stem from the traction-free conditions on the macro-crack faces $\theta = \pm\pi$, while the last condition is introduced here arbitrarily for the purpose of normalizing $\bar{F}(\theta)$. For $\omega = 0$, the nonlinear eigenvalue problem reduces to that of Mode III HRR-field. It can be easily shown that the eigenvalue s takes the same value as the HRR-field, i.e.,

$$s = n/(n+1), \tag{22}$$

With Eq. (22), the first boundary condition of (21) is identically satisfied. Consequently, the differential equation (16) in conjunction with the remaining two boundary conditions at $\theta = -\pi$ can be regarded as an initial value problem for determining the eigenfunction $\bar{F}(\theta)$. In this analysis, the initial value problem is solved numerically by a fourth-order Runge-Kutta method. Once s and $\bar{F}(\theta)$ have been determined, all other field quantities can be immediately obtained by using Eqs. (14) and (15), as well as the constitutive equations (7).

One important feature of the constitutive equations (7) is that they do not destroy the path-independence of the J-integral (Rice, 1968). This enables to use J as a crack-tip characterizing paramter, and to relate it to the amplitude factor A appearing in Eq. (13) by

$$J = \alpha\gamma_0\tau_0 A^{n+1} I_n, \tag{23}$$

where I_n is a normalization constant. Substitution of Eq. (23) into Eqs. (14) and (15) and subsequently into the constitutive equations (7) yields the following asymptotic expressions for the crack-tip field

$$\begin{Bmatrix} \tau_r \\ \tau_\theta \\ \tau_e \end{Bmatrix} = \tau_0\left(\frac{J}{\alpha\gamma_0\tau_0 I_n r}\right)^{\frac{1}{n+1}} \begin{Bmatrix} \bar{\tau}_r(\theta) \\ \bar{\tau}_\theta(\theta) \\ \bar{\tau}_e(\theta) \end{Bmatrix}, \tag{24}$$

$$\begin{Bmatrix} \gamma_r \\ \gamma_\theta \\ \gamma_e \end{Bmatrix} = \alpha\gamma_0\left(\frac{J}{\alpha\gamma_0\tau_0 I_n r}\right)^{\frac{n}{n+1}} \begin{Bmatrix} \bar{\gamma}_r(\theta) \\ \bar{\gamma}_\theta(\theta) \\ \bar{\gamma}_e(\theta) \end{Bmatrix}, \tag{25}$$

$$w = \alpha\gamma_0 r^{\frac{1}{n+1}}\left(\frac{J}{\alpha\gamma_0\tau_0 I_n}\right)^{\frac{n}{n+1}}\bar{w}(\theta), \tag{26}$$

where

$$\bar{\tau}_r = -\bar{F}', \qquad \bar{\tau}_\theta = n\bar{F}/(n+1), \qquad \bar{\tau}_e = (\bar{\tau}_r^2 + \bar{\tau}_\theta^2)^{1/2}. \tag{27}$$

$$\bar{\gamma}_r = \bar{\tau}_e^{n-1}[\bar{\tau}_r - p(\theta)], \qquad \bar{\gamma}_\theta = \bar{\tau}_e^{n-1}[\bar{\tau}_\theta + q(\theta)], \qquad \bar{\gamma}_e = (\bar{\gamma}_r^2 + \bar{\gamma}_\theta^2)^{1/2}, \tag{28}$$

$$\bar{w} = (n+1)\bar{\gamma}_r. \tag{29}$$

Note here that the crack-tip field (24)-(26) has exactly the same structure as the HRR-field for a Mode III crack (Hutchinson, 1968; Rice and Rosengren, 1968). The angular functions and the normalization constant I_n differ, however, from those of the HRR-field, due to the presence of dispersed micro-cracks. Following the usual definition (Tracey, 1976) for the crack opening displacement δ_t, the following relation between the crack opening displacement δ_t and the J-integral holds

$$\delta_t = d_n\frac{J}{\tau_0}, \qquad d_n = \frac{2\gamma_0}{I_n}[\bar{w}(\pi)]^{\frac{n+1}{n}}. \tag{30}$$

RESULTS

For n=10 and for $\phi = 0°$ and $90°$, numerical results for the angular functions of the crack-tip field are presented in Figs. 2 and 3 versus the polar angle θ and the damage parameter ω. The maximum value of $\bar{\tau}_e(\theta)$ in the interval $-\pi \leq \theta \leq \pi$ is taken to be unity for the purpose of normalization, i.e.,

$$\max \bar{\tau}_e(-\pi \leq \theta \leq \pi) = 1\,. \tag{31}$$

The contours of constant effective shear stress τ_e are also shown in Figs. 2 and 3. Here, a dimensionless polar coordinate $R(\theta)$ is introduced as

$$R(\theta) = (\frac{\tau_e}{\tau_0})^{n+1}(\frac{\alpha\gamma_0\tau_0}{J})r = \frac{1}{I_n}\bar{\tau}_e^{n+1}(\theta)\,. \tag{32}$$

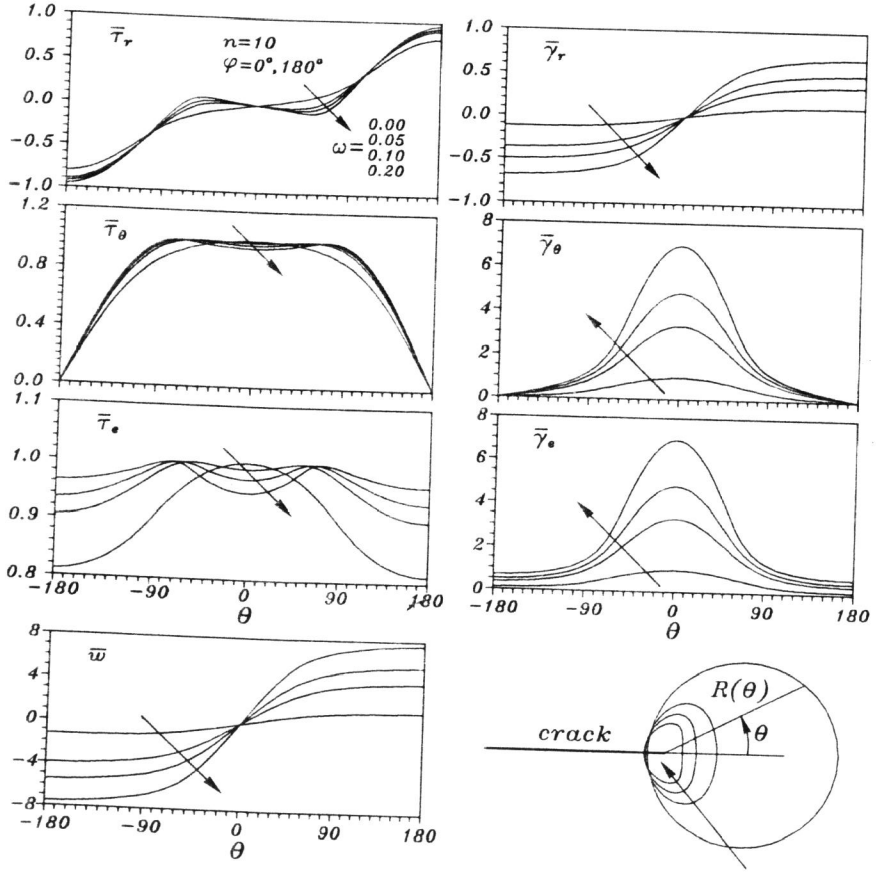

Figure 2: Angular functions and contours of constant τ_e (θ in degrees)

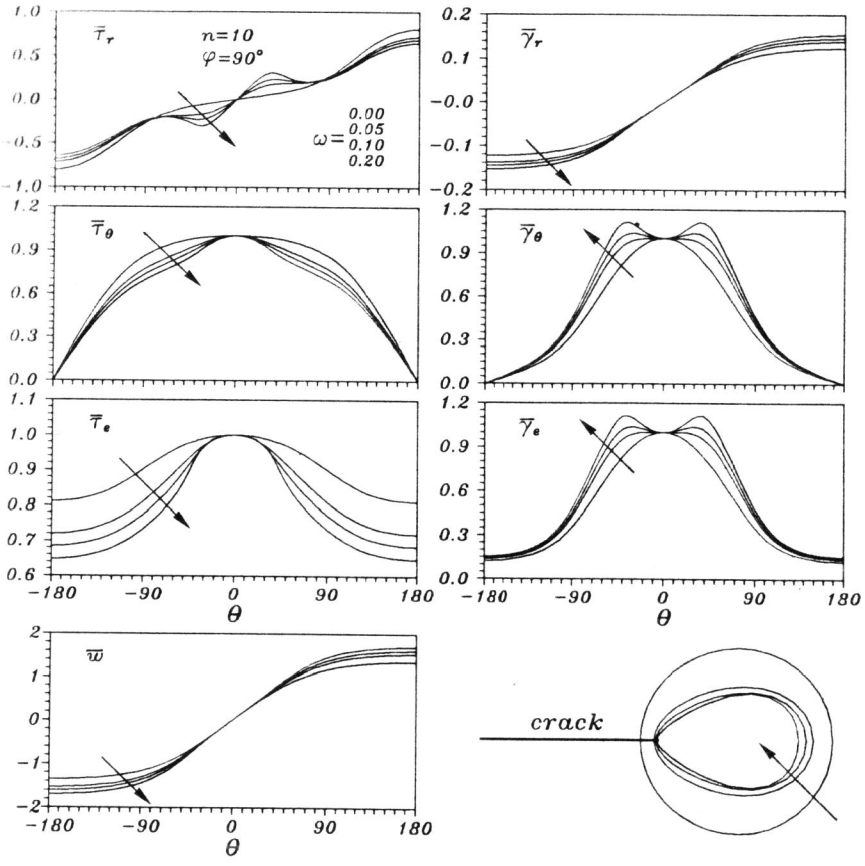

Figure 3: Angular functions and contours of constant τ_e (θ in degrees)

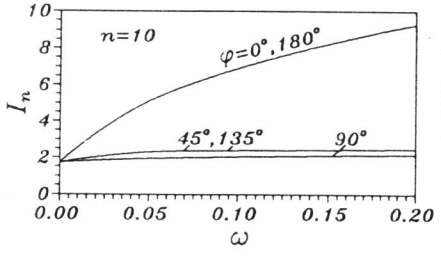

Figure 4: I_n versus ω

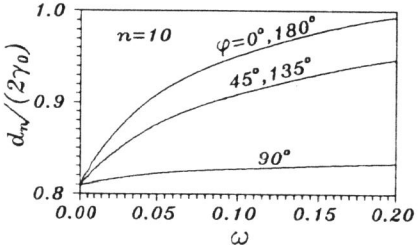

Figure 5: $d_n/(2\gamma_0)$ versus ω

Figures 2 and 3 indicate that the angular functions $\bar{\tau}_r$ and $\bar{\tau}_\theta$ are only weakly dependent on the damage parameter ω, while $\bar{\tau}_e$ is strongly affected by ω. In the presence of damage and for $\phi = 0^o$, the maximum $\bar{\tau}_e$ doesn't appear on the crack line ahead of the macro-crack tip. Near the crack faces ($\theta = \pm\pi$) and for fixed θ, $\bar{\tau}_e$ increases with increasing ω for $\phi = 0^o$, while this feature is reversed for $\phi = 90^o$. The influence of ω on $\bar{\gamma}_r$, $\bar{\gamma}_\theta$ and $\bar{\gamma}_e$ is stronger for $\phi = 0^o$ than for $\phi = 90^o$. The presence of micro-cracks gives rise to increases in $\bar{\gamma}_\theta$ and $\bar{\gamma}_e$, and the increases are larger for larger ω. For $\phi = 90^o$, the position of the maximum $\bar{\gamma}_\theta$ and $\bar{\gamma}_e$ is no longer on the crack line, i.e., $\theta = 0^o$. The maximum $\bar{w}$ increases with increasing ω. For fixed θ and ω, the increase in $\bar{w}$ is larger for $\phi = 0^o$ than for $\phi = 90^o$. The effect of ω on $\bar{w}$ is minimal when the micro-cracks are perpendicular to the macro-crack, i.e., $\phi = 90^o$. The largest dimension of $R(\theta)$ is reduced by the presence of damage, and for a given ϕ the reduction increases as ω increases. For the cases considered here, the maximum reduction of $R(\theta)$ is attained at $\phi = 0^o$. The shape of the contours of constant τ_e is also altered by the micro-cracks, and it is no longer a circle for $\omega \neq 0$.

The dependence of the normalization constant I_n on the damage parameter ω is shown in Fig. 4, for several micro-crack orientations ϕ. It is seen on Fig. 4 that I_n increases with increasing ω. The increase of I_n is strongest for $\phi = 0^o$ and 180^o and weakest for $\phi = 90^o$. Figure 5 presents the variation of $d_n/(2\gamma_0)$ with the damage parameter ω, where d_n relates the crack opening displacement δ_t to the J-integral via Eq. (30). Figure 5 reveals that the presence of distributed micro-cracks increases $d_n/(2\gamma_0)$ and consequently the crack opening displacement δ_t (for a given J). The larger ω is, the larger is $d_n/(2\gamma_0)$. The largest magnification in $d_n/(2\gamma_0)$ is induced when the micro-cracks are parallel to the macro-crack, i.e., when $\theta = 0^o$ and 180^o.

REFERENCES

1 Abeyaratne, R. (1983): On the Estimation of Energy Release Rates. *ASME J. Appl. Mech.*, **50**, 19-23.

2 Amazigo, J. C. (1974): Fully Plastic Crack in an Infinite Body Under Anti-Plane Shear. *Int. J. Solids Structures*, **10**, 1003-1015.

3 He, M. Y. (1987): Perturbation Solutions on J-Integral for Nonlinear Crack Problems. *ASME J. Appl. Mech.*, **54**, 240-242.

4 Hutchinson, J. W. (1968): Singular Behavior at the End of a Tensile Crack in a Hardening Material. *J. Mech. Phys. Solids*, **16**, 13-31.

5 Rice, J. R. and Rosengren, G. F. (1968): Plane Strain Deformation Near a Crack Tip in a Power-Law Hardening Material. *J. Mech. Phys. Solids*, **16**, 1-12.

6 Rice, J. R. (1968): A Path Independent Integral and the Approximate Analysis of Strain Concentrations by Notches and Cracks. *ASME J. Appl. Mech.*, **35**, 379-386.

7 Tracey, D. M. (1976): Finite Element Solutions for Crack Tip Behavior in Small-Scale Yielding. *ASME J. Engng. Mater. Tech.*, **98**, 146-151.

8 Zhang, Ch. and Gross, D. (1991): Das Rissspitzenfeld beim stabilen Rissfortschritt unter Berücksichtigung der Schädigungsentwicklung. Institute of Mechanics, TH Darmstadt, Germany. Report Nr. 3/91.